

Investigation of some oleochemicals as green inhibitors on mild steel corrosion in sulfuric acid

M. Z. A. Rafiquee · Sadaf Khan · Nidhi Saxena ·
M. A. Quraishi

Received: 8 July 2008 / Accepted: 27 January 2009 / Published online: 14 February 2009
© Springer Science+Business Media B.V. 2009

Abstract The inhibitive effect of four oleo chemicals (namely; 2-Pentadecyl-1,3-imidazoline (PDI), 2-Undecyl-1,3-imidazoline (UDI), 2-Heptadecyl-1,3-imidazoline (HDI), 2-Nonyl-1,3-imidazoline (NI)), regarded as green inhibitors, were studied for the corrosion protection of mild steel in 0.5 M H₂SO₄. The methods employed were weight loss, potentiodynamic polarization and electrochemical impedance techniques. Scanning electron microscopy (SEM) was carried out on the inhibited and uninhibited metal samples to characterize the surface. The purity of synthesized inhibitors was checked by FT-IR and NMR studies. The inhibition efficiency increased with increase in inhibitor concentration, immersion time and decreased with increase in solution temperature. No significant change in IE values was observed with increase in acid concentration. The best performance was obtained for UDI possessing 96.2% inhibition efficiency at 500 ppm concentration. The adsorption of the compounds on the mild steel surface in the presence of sulfuric acid obeyed Langmuir's adsorption isotherm. The values obtained for free energy of adsorption and heats of adsorption suggest physical adsorption. The addition of inhibitor decreased the entropy of activation suggesting that the inhibitors are more orderly arranged along the mild steel surface. The potentiodynamic polarization data indicate mixed control. The electrochemical impedance study further confirms the formation of a

protective layer on the mild steel surface through the inhibitor adsorption.

Keywords Corrosion and oxidation · Metals and alloys · Kinetics · Surfaces · Thin films · Green inhibitors

1 Introduction

Heterocyclic compounds represent a potential class of corrosion inhibitors. Nitrogen-based heterocyclic compounds are effective inhibitors for mild steel corrosion in acidic solutions [1–3]. The presence of the lone pair of electrons on the nitrogen atoms helps to delocalize the electrons and thus stabilize the compound. The heterocyclic nitrogen is adsorbed onto the metal surface through electrostatic interactions between the electron deficient nitrogen atom and the electron rich metal surface [4].

Compounds derived from fatty acids constitute an important class of corrosion inhibitor [5, 6]. They are used [7] in oil wells and pipelines and in the gas industry. Compounds containing the imidazoline ring have displayed good corrosion inhibiting behavior on copper [8, 9] and mild steel [10] in acid media.

The influence of some oleo chemicals namely, 2-Nonyl-1,3-imidazoline (NI), 2-Undecyl-1,3-imidazoline (UDI), 2-Pentadecyl-1,3-imidazoline (PDI), 2-Heptadecyl-1,3-imidazoline (HDI), regarded as green inhibitors, on the corrosion of mild steel in 0.5 M H₂SO₄ were studied and are reported here. The selection of these inhibitors is based on the fact that these compounds can be synthesized conveniently from relatively cheap raw materials. The presence of non-bonded electron pairs on the nitrogen atom induces greater adsorption of the compounds onto the metal surface thus providing higher inhibition efficiency.

M. Z. A. Rafiquee (✉) · S. Khan · N. Saxena
Corrosion Research Laboratory, Department of Applied
Chemistry, Faculty of Engineering and Technology,
Aligarh Muslim University, Aligarh 20 2002, India
e-mail: drrafiquee@gmail.com

M. A. Quraishi
Department of Applied Chemistry, Institute of Technology,
Banaras Hindu University, Varanasi 221 005, India

2 Experimental details

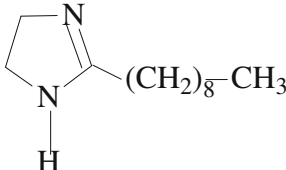
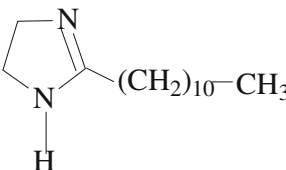
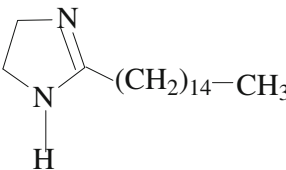
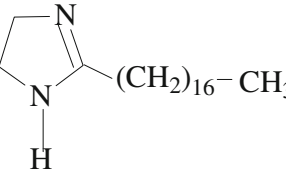
Weight loss experiments were performed with cold rolled mild steel strips of size $2.0 \times 2.5 \times 0.05 \text{ cm}^3$ having composition (wt%); 0.14% C, 0.35% Mn, 0.17% Si, 0.025% S, 0.03% P, and balance Fe as per a standard method [11]. Double distilled water was used to prepare solutions of 0.5 M H_2SO_4 . Imidazolines were synthesized by the procedure described by Hofmann [12] and were characterized through their spectral data; the purity was confirmed by thin layer chromatography, FT-IR (Model No Interspec 2020, UK) & NMR (Bruker spectrosSpin 300 MHz) study. FT-IR spectra of imidazoline derivative were obtained in KBr using a Fourier transform spectrometer. The name, molecular structure and molecular weight of the compounds are given in Table 1. The weight loss was monitored using an electronic balance (Model no. Precisa 205 A SCS) after dipping the mild steel strips in 0.5 M H_2SO_4 medium. The potentiodynamic

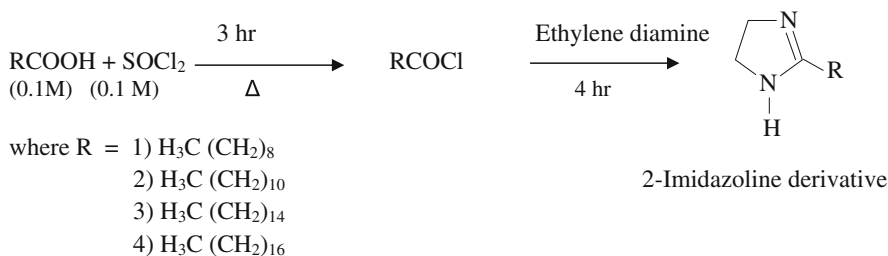
polarization studies was performed on EG & G PARC potentiostat/galvanostat (model 173), universal programmer (model 175) and X – Y recorder (model RE 0089). The electrochemical impedance was recorded on a Zahner IM-6 electrochemical workstation. Scanning electron micrographs of the mild steel surface were taken before and after using the imidazoline inhibitor (Model No 435 VP LEO).

2.1 Synthesis of imidazoline derivatives

An appropriate amount of respective fatty acid (0.1 M) was dissolved in 50 mL absolute alcohol and treated with thionyl chloride (0.1 M). The mixture was refluxed for 3 h. The reaction product was then treated with ethylene diamine (6 mL) and refluxed for a further 4 h as presented in Scheme 1. After completion of the reaction, the solution was filtered, washed with water, dried and then crystallized in ethanol.

Table 1 Name, structural formula and relative molecular weights of the imidazolines used

S.No.	Structure	Name and abbreviation	Relative mol. weight
1.		2-Nonyl-1, 3-imidazoline (NI)	248
2.		2-Undecyl-1, 3-imidazoline (UDI)	276
3.		2-Pentadecyl-1, 3-imidazoline (PDI)	332
4.		2-Heptadecyl-1, 3-imidazoline (HDI)	360

Scheme 1 Synthesis of imidazolines

2.2 Electrochemical impedance studies

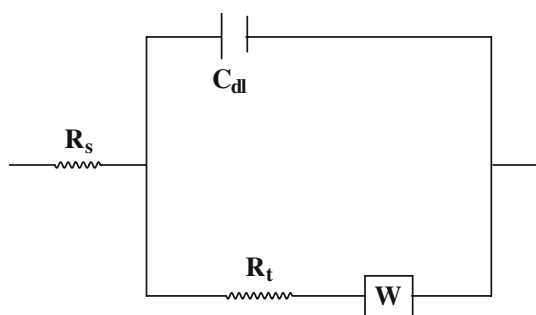
The electrical equivalent circuit for the system is shown in Fig. 1.

The values of R_t and C_{dl} were obtained using the Nyquist plot [13]. The %IE was calculated from the following equation [14]:

$$\text{IE \%} = \frac{1/R_o - 1/R_t}{1/R_o} \times 100 \quad (1)$$

where, R_t and R_o are the charge transfer resistance with and without inhibitor, respectively.

The measurements were carried out using a Zahner IM-6 electrochemical workstation at 30 ± 2 °C, in the frequency range 5 Hz–100 kHz at E_{corr} for mild steel in 0.5 M H₂SO₄.



- R_s = Solution resistance,
 R_t = charge transfer resistance,
 W = Warburg impedance,
 C_{dl} = Double layer capacitance.

Fig. 1 Electrical equivalent circuit for the system (R_s = solution resistance, R_t = charge transfer resistance, C_{dl} = double layer capacitance, W = Warburg impedance)

2.3 Scanning electron microscopy

The specimen after immersion for 2 h at room temperature was thoroughly washed with doubly distilled water before putting on the slide. The photographs were taken from that portion of the specimen where better information was expected. The following cases were examined.

- Polished mild steel specimen
- Mild steel specimen immersed in 0.5 M H₂SO₄
- Mild steel specimen immersed in 0.5 M H₂SO₄ containing 500 ppm of UDI.

3 Results and discussion

3.1 FT-IR spectroscopy

The detail of the different stretching frequencies observed due to the presence of (C=N), (C–N), (C–H), (N–H), (CH₃) groups in the molecules are given in Table 2. It is clear that the synthesized compounds are the same as predicted by the reaction given in Scheme 1.

3.2 NMR spectroscopy

The presence of different types of protons in 2-Undecyl-1, 3-imidazoline (UDI) were confirmed by the NMR Spectral data (δCDCl_3) and the values obtained were at 7.350 (1H, NH), 1.936 (20H (CH₂)₁₀), 1.253 (3H, CH₃), 2.006 (4H, (CH₂)₂).

3.3 Weight loss

The weight loss experiments were carried out at 30 °C temperature with immersion time 2 h at the different

Table 2 Stretching frequencies of the synthesized inhibitors (using KBr)

Name of inhibitor	C=N cm ⁻¹	C–N cm ⁻¹	C–H cm ⁻¹	N–H cm ⁻¹	CH ₃ cm ⁻¹
2-Nonyl-1, 3-imidazoline (NI)	1648	1352	2924	3146	1172
2-Undecyl-1, 3-imidazoline (UDI)	1647	1323	2852	3257	1166
2-Pentadecyl-1, 3-imidazoline (PDI)	1640	1463	2845	3290	1164
2-Heptadecyl-1, 3-imidazoline (HDI)	1665	1372	2845	2921	1250

concentrations of inhibitor and sulfuric acid. The weight loss was also monitored as a function of varying temperature (in the range of 30–60 °C) and immersion time (2–24 h) at fixed temperature (30 °C) and inhibitor (500 ppm) and sulfuric acid concentration (0.5 M). The percentage inhibition efficiencies (%IE) and corrosion rates (CR) are summarized in Table 3. All the compounds inhibited the corrosion of mild steel in H₂SO₄ at each concentration used i.e., 25–700 ppm.

The percentage inhibition efficiency (IE) was calculated using the equation:

$$\text{IE \%} = \frac{\text{CR}_0 - \text{CR}}{\text{CR}_0} \times 100 \quad (2)$$

where, CR₀ and CR are the corrosion rates in the absence and presence of inhibitor, respectively.

The variation of inhibition efficiency with inhibitor concentration is shown in Fig. 2a. The inhibition efficiency increased with increase in concentration up to 500 ppm;

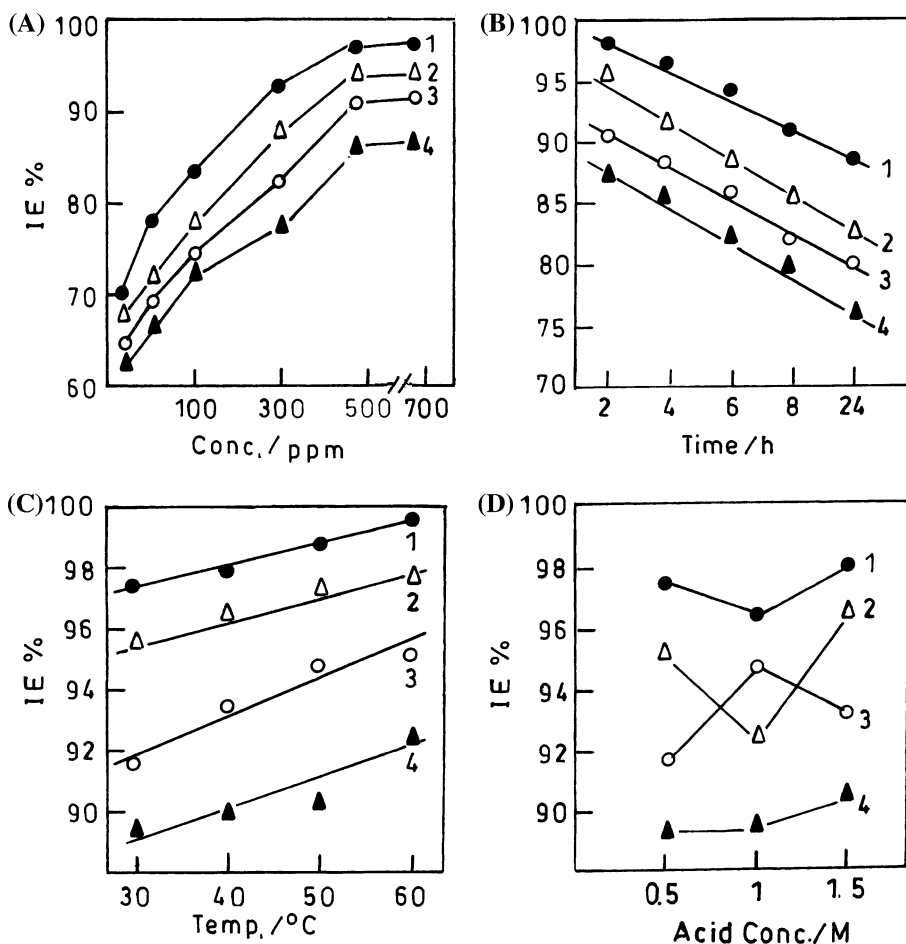
thereafter further increase did not enhanced the IE significantly. The maximum IE was achieved at 500 ppm. The effect of immersion time on IE is shown in Fig. 2b. IE decreased with increase in immersion time from 2 to 24 h in the presence of inhibitor. The decrease in inhibition efficiency with time may be attributed to increase in cathodic reaction or increase in ferrous ion concentration [15]. IE increases with the increase in temperature from 30 to 60 °C (Fig. 2c) indicating that an imidazoline film is formed due to adsorption in this temperature range [16]. This shows the persistence of the adsorbed fatty acid imidazolines over a longer test period. Studies on the variation of IE with acid concentration (Fig. 2d) demonstrate that there is no significant change in IE with increase in acid concentration from 0.5 to 1.5 M H₂SO₄. Thus the imidazolines behave as effective inhibitors even in higher acid concentrations [17].

The degree of surface coverage (θ) in the presence of inhibitor at different concentrations (in the range

Table 3 Corrosion parameters for mild steel in aqueous solution of 0.5 M H₂SO₄ in absence and presence of different concentrations of various inhibitors from weight loss measurements at 30 °C for 2 h

Inhibitor concentration (ppm)	Weight loss (mg)	IE (%)	CR (mm year ⁻¹)
0.5 M H ₂ SO ₄	108.00	–	60.18
UDI			
25	32.22	70.16	17.95
50	23.25	78.47	12.96
100	17.23	84.05	9.60
300	8.01	92.58	4.47
500	2.77	97.43	1.54
700	4.16	96.15	2.32
NI			
25	34.30	68.24	19.11
50	28.99	73.15	16.16
100	23.09	78.62	12.87
300	13.57	87.43	7.56
500	5.23	95.16	2.91
700	6.24	94.22	3.47
PDI			
25	37.35	65.42	20.81
50	31.44	70.89	17.52
100	26.32	75.63	14.67
300	17.92	83.41	9.98
500	8.78	91.87	4.89
700	10.42	90.35	5.81
HDI			
25	40.02	62.94	22.30
50	34.74	67.83	19.36
100	29.41	72.77	16.39
300	22.15	79.49	12.34
500	19.91	87.20	5.54
700	15.58	85.57	8.68

Fig. 2 Variation of inhibition efficiency with (a) inhibitor concentration, (b) immersion time, (c) solution temperature, (d) acid concentration in 0.5 M H₂SO₄ (1: UDI; 2: NI; 3: PDI; 4: HDI)



25–700 ppm) at 30 °C after immersion for 2 h in 0.5 M H₂SO₄ was evaluated from weight loss data. The data were tested graphically by fitting to various isotherms e.g. Temkin, Langmuir, Freundlich etc. A straight line with R^2 values 0.8238 for UDI, 0.9773 for NI, 0.9857 for PDI and 0.9736 for HDI was obtained for $\log(\theta/1 - \theta)$ versus $1/T$ (Fig. 3a). From the slope ($= -Q/2.303 R$) of the plot the values of heat of adsorption (Q) were obtained and are given in Table 4. The lower negative values of heat of adsorption indicate physical adsorption [18].

A plot of \log of corrosion rate versus $1/T$, as obtained by weight loss measurement, gave a straight line ($R^2 = 0.8769$ for UDI, 0.8956 for NI, 0.8751 for PDI, 0.8424 for HDI) as shown in Fig. 3b. This behavior is in accordance with work of other authors [19–21] who proposed the following relationship (Arrhenius equation) to calculate the energy of activation:

$$\text{Log(Corrosion Rate)} = \frac{-E_a^0}{2.303RT} + A \tag{3}$$

where, E_a^0 is the apparent effective activation energy, R the gas constant and A the Arrhenius pre-exponential factor.

The values of activation energy (E_a^0) obtained from the slope are given in Table 4. An alternative formula for the Arrhenius equation is the transition state equation:

$$\text{Corrosion Rate} = \frac{RT}{Nh} \exp\left(\frac{\Delta S^0}{R}\right) \exp\left(-\frac{\Delta H^0}{RT}\right) \tag{4}$$

where, h is the Plank constant, N the Avogadro number, ΔS^0 the change in entropy of activation, and ΔH^0 the change in enthalpy of activation. A plot of $\log(CR/T)$ versus $1/T$ gave a straight line with R^2 ($=0.9234$ for UDI, 0.9821 for NI, 0.8799 for PDI, 0.8575 for HDI), as shown in Fig. 3c. From the slope ($= -\Delta H^0/2.303 R$) and intercept ($= [(\log(R/Nh) + (\Delta S^0/2.303 R))]$) the values of ΔH^0 and ΔS^0 were calculated. The values of thermodynamic activation parameter (E_a^0) for the corrosion of mild steel in 0.5 M H₂SO₄ solution are lower in the presence of the inhibitor than in its absence. This indicates that the inhibitors are effective at elevated temperatures [22]. The values of change in activation entropy, ΔS^0 , in the presence of the inhibitor are large and negative indicating that the activated complex in the rate determining step is associative in nature and,

Fig. 3 Plots of (a) $\log(\theta/1-\theta)$ versus $1/T$; (b) $\log(CR)$ versus $1/T$; (c) $\log(CR/T)$ versus $1/T$; and (d) $\log(\text{weight loss})$ versus immersion time in 0.5 M H_2SO_4 (1: UDI; 2: NI; 3: PDI; 4: HDI; 5: Blank)

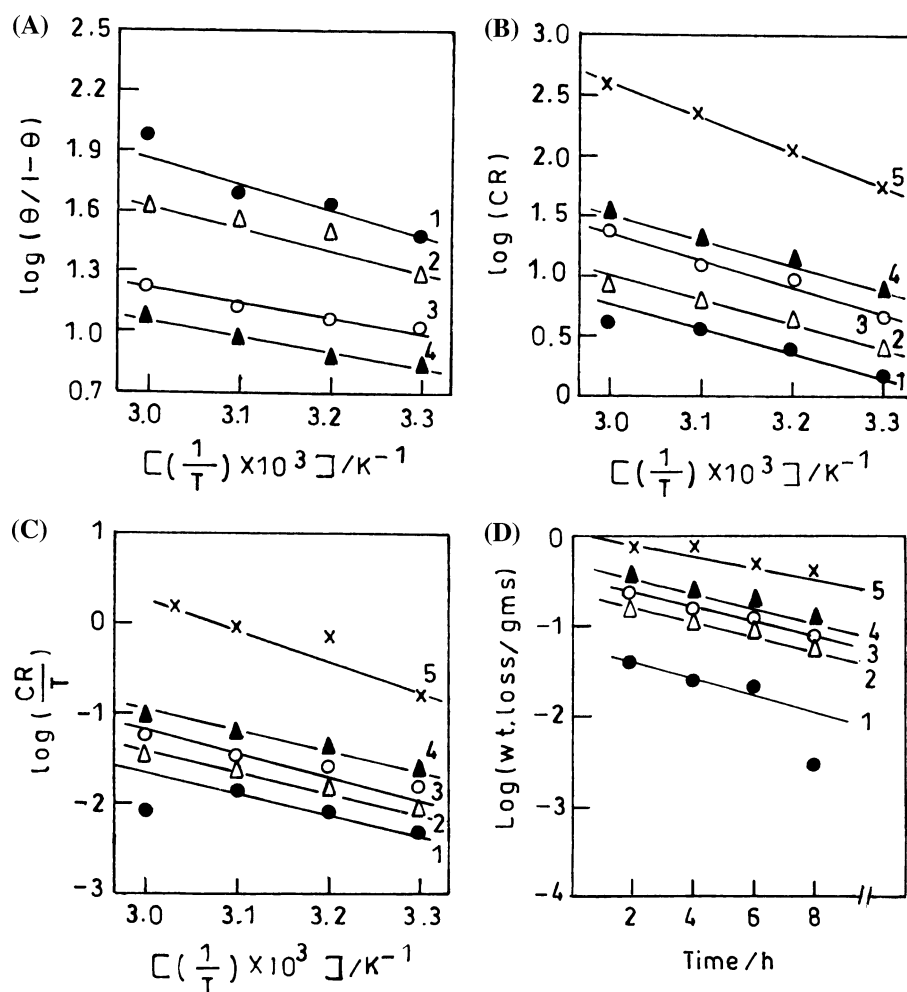


Table 4 Thermodynamic activation parameters for mild steel in 0.5 M H_2SO_4 in the absence and presence of inhibitors of 500 ppm concentration

System	E_a (kJ mol ⁻¹)	$-\Delta H$ (kJ mol ⁻¹)	$-\Delta S$ (J mol ⁻¹ K ⁻¹)	$-\Delta G_{ads}$ (kJ mol ⁻¹)	$-Q$ (kJ mol ⁻¹)
0.5 M H_2SO_4	57.33	57.40	197.59	–	–
UDI	45.95	47.86	214.83	38.59	28.70
NI	44.04	46.14	218.66	35.98	26.81
PDI	41.36	44.61	222.49	34.98	16.60
HDI	38.87	38.29	228.23	33.91	15.95

therefore, the activated complex has more orderly structure [23]. The change in the values of free energy of adsorption (ΔG_{ads}) calculated using the following equations [24], are given in Table 4.

$$\Delta G_{ads} = -RT \ln(55.5K) \quad (5)$$

where, K is given by:

$$K = \theta/C(1-\theta) \quad (6)$$

In this equation, C is the concentration of inhibitor in mol dm⁻³, K is the equilibrium constant. The negative and

lower values of ΔG_{ads} indicate that the adsorption of inhibitor on the mild steel surface is spontaneous and physical in nature [25].

The weight loss was monitored as a function of immersion time at constant inhibitor and acid concentrations at 30 °C. The rate constant for the dissolution of metal in acidic medium was calculated by employing the first order rate law (Eq. 7). The constant value of k at different immersion times indicates first order kinetics. A straight line plot of $\log(\text{weight loss})$ versus Immersion time is shown in Fig. 3d [26].

$$k = \frac{2.303}{t} \log \frac{[A_o]}{[A]} \tag{7}$$

where, $[A_o]$ is the initial weight of the metal and $[A]$ is the weight loss corresponding to immersion time t . The half-life ($t_{1/2}$) was calculated using the Eq. 8 [27].

$$t_{1/2} = 0.693/k \tag{8}$$

The values of rate constants and half-life period ($t_{1/2}$) obtained from the above equations are summarized in Table 5. The half-life values indicate the durability of the inhibitor [28]. The inhibitor effectiveness followed the order; UDI > NI > PDI > HDI.

3.4 Adsorption isotherm

The degrees of surface coverage (θ) were evaluated from weight-loss data. A plot of $\log \theta/(1 - \theta)$ vs. $\log C$ gave a straight line (Fig. 4a) ($R^2 = 0.9374, 0.897, 0.9286, 0.9417$ for UDI, NI, PDI, HDI, respectively) indicating that the adsorption follows the Langmuir isotherm. To confirm the Langmuir adsorption isotherm, a plot of C/θ vs. C was plotted (Fig. 4b) ($R^2 = 0.9972, 0.9969, 0.9977, 0.9993$ for UDI, NI, PDI, HDI, respectively).

$$\theta/(1 - \theta) = kC \exp(-\Delta G_{ads}/RT) \tag{9}$$

where ΔG_{ads} is the change in free energy of adsorption.

3.5 Potentiodynamic polarization

The cathodic and anodic polarization curves of mild steel in 0.5 M H_2SO_4 in the absence and presence of inhibitor at 500 ppm concentration at 28 ± 2 °C are shown in Fig. 5. The electrochemical parameters corrosion current density (I_{corr}), corrosion potential (E_{corr}) and % IE were calculated from the Tafel plots and are given in Table 6. A maximum decrease in I_{corr} was observed for UDI. E_{corr} values show that all these compounds are mixed type inhibitors in sulfuric acid medium.

Table 5 First order rate constant and Half-life values in hours (h) for the corrosion of mild steel in 0.5 M H_2SO_4 in absence and presence of inhibitors of 500 ppm concentration at 30 °C

System	$10^{-3} k$ (h^{-1})	$t_{1/2}$ (h)
0.5 M H_2SO_4	49.60 ± 0.126	13.87
UDI	2.078 ± 0.0027	333.49
NI	4.320 ± 0.0052	160.42
PDI	5.220 ± 0.0064	132.76
HDI	7.490 ± 0.0086	92.52

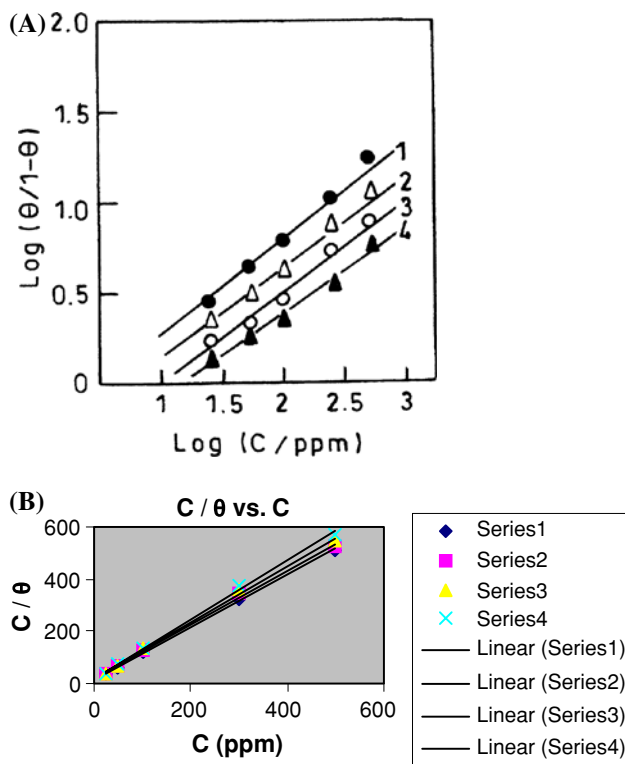


Fig. 4 a Langmuir adsorption isotherm plots for $\log [\theta/(1 - \theta)]$ versus $\log C$ for the adsorption of various inhibitors on the surface of mild steel in 0.5 M H_2SO_4 (1: UDI; 2: NI; 3: PDI; 4: HDI). b Langmuir adsorption isotherm plots for C/θ versus C for the adsorption of various inhibitors on the surface of mild steel in 0.5 M H_2SO_4 (Series 1: HDI; Series 2: PDI; Series 3: NI; Series 4: UDI)

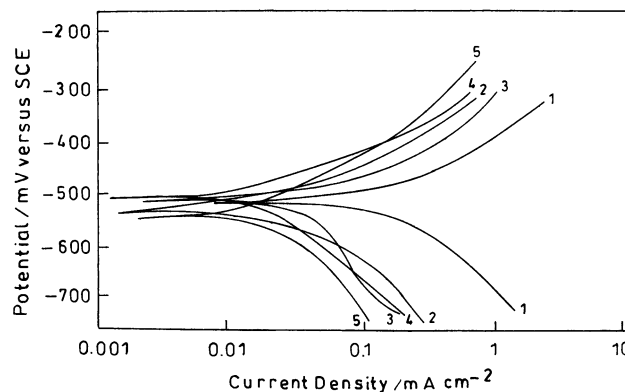


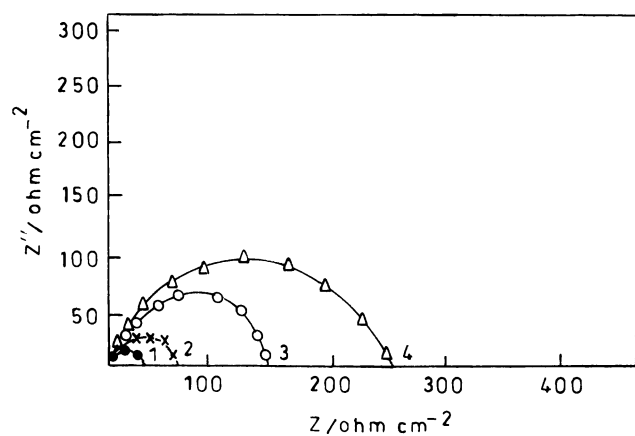
Fig. 5 Potentiodynamic polarization curves for mild steel containing 500 ppm imidazolines in 0.5 M H_2SO_4 (1: Blank; 2: HDI; 3: PDI; 4: NI; 5: UDI)

3.6 Electrochemical impedance study

The impedance diagram does not give a perfect semicircle and this has been attributed to frequency dispersion [29]. The impedance diagram for mild steel in 0.5 M H_2SO_4 is shown in Fig. 6 and the values of R_r , C_{dl} and % IE are given in Table 7. The values of R_i increase with increase in

Table 6 Electrochemical polarization parameters for the corrosion of mild steel in 0.5 M H₂SO₄ containing 500 ppm inhibitors at 30 °C

System	E_{corr} (mV)	I_{corr} (mA cm ⁻²)	IE (%)
0.5 M H ₂ SO ₄	-533.00	0.360	-
UDI	-538.00	0.017	95.32
NI	-526.00	0.025	93.08
PDI	-520.00	0.044	87.54
HDI	-542.00	0.057	84.16

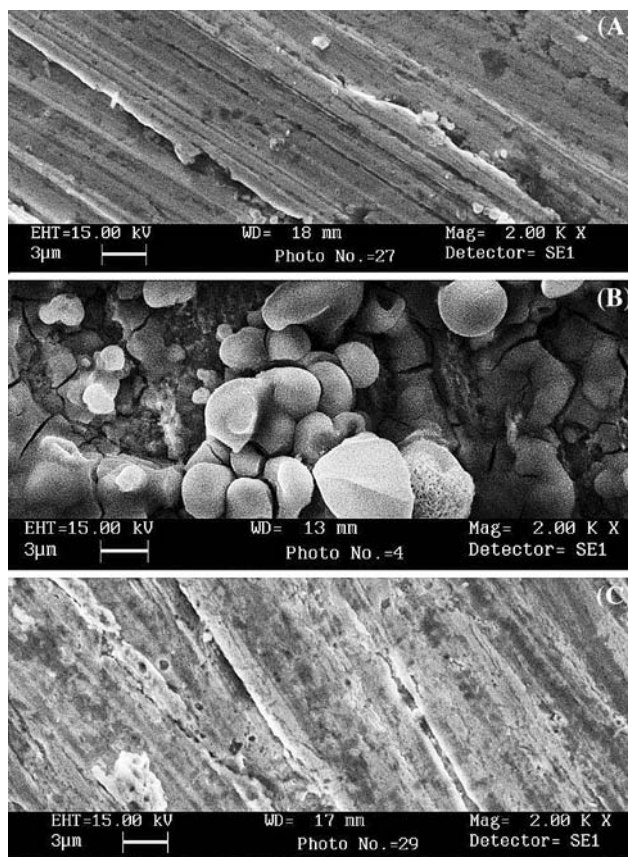
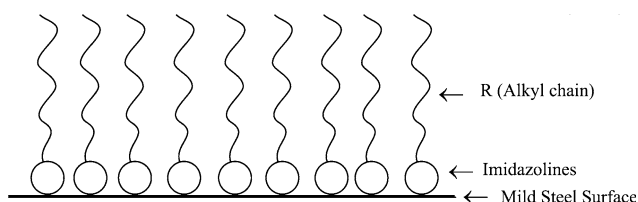
**Fig. 6** Electrochemical impedance diagram (Nyquist plot) for mild steel in 0.5 M H₂SO₄ in the absence and presence of UDI at different concentrations (1: Blank; 2: 25 ppm; 3: 100 ppm; 4: 500 ppm)**Table 7** Electrochemical impedance parameters for the corrosion of mild steel in 0.5 M H₂SO₄ containing different concentrations of UDI at 30 °C

System	R_t (ohm cm ²)	C_{dl} (μF cm ⁻²)	IE (%)
0.5 M H ₂ SO ₄	17.00	4.67	-
UDI			
25	61.73	2374.00	72.43
100	128.84	1000.00	86.80
500	260.48	380.19	93.47

inhibitor concentration and the reverse behavior is observed for C_{dl} values; this, in turn, leads to an increase in % IE [30]. These data agree with the weight loss and SEM studies suggesting that inhibition is attributable to surface adsorption of the inhibitor [31].

3.7 Scanning electron microscopy

Scanning electron photographs of the metal sample in the presence and absence of inhibitor are shown in Fig. 7. The inhibited metal surface is smoother than the uninhibited surface indicating a protective layer of adsorbed inhibitor preventing acid attack [32].

**Fig. 7** Scanning electron micrographs of (a) Polished mild steel (b) After immersion in 0.5 M H₂SO₄ for 2 h (c) After immersion in 0.5 M H₂SO₄ for 2 h with 500 ppm UDI**Fig. 8** Diagram of adsorption of imidazolines on the steel surface

3.8 Mechanism of corrosion inhibition

The protonated imidazolines in the presence of sulfuric acid medium are adsorbed on the metallic surface through the ring [33]. The hydrocarbon chain also prevents the acid attack. The schematic binding of the imidazole ring to the metal surface is presented in Fig. 8. The imidazolines are bound to the surface through the head of the molecule. The increase in chain length of the alkyl group increases the molecular weight of imidazoline and, thereby, decreases the number of molecules containing imidazole ring in a fixed weight (500 ppm) of inhibitor; therefore, the inhibition efficiency is decreased. The higher inhibition efficiency of NI and UDI may be due to their being the

least hydrophobic among the tested imidazolines, therefore having a greater tendency to adsorb.

4 Conclusions

- (1) The oleo compounds acted as efficient corrosion inhibitor in H₂SO₄ acid medium.
- (2) Adsorption of imidazolines on mild steel in H₂SO₄ solution obeyed the Langmuir adsorption isotherm.
- (3) The imidazolines behave as mixed type inhibitors in H₂SO₄ solution.
- (4) UDI inhibitor increases R_p values and decreases C_{dl} values showing that inhibition takes place by adsorption.

Acknowledgements The authors thank the Chairman, Department of Applied Chemistry, for facilities provided during the research and one of the authors (S.K) is thankful to the Council of Scientific and Industrial Research (C.S.I.R), New Delhi for the award of a Senior Research Fellowship (File no. 09/112(0407)2K8-EMR-I).

References

1. Noor EA (2005) *Corros Sci* 47:33
2. Samardzija KB, Khaled KF, Hackerman N (2005) *Anti Corros Met Mater* 52:11
3. Lebrini M, Lagrenee M, Traisnel M, Gengembre L, Vezin H, Bentiss F (2007) *Appl Surf Sci* 25:9267
4. Kartritzky AR (2005) *Advances in heterocyclic chemistry*. Elsevier, San Diego, p 84
5. Quraishi MA, Ansari FA (2006) *J Appl Electrochem* 36:309
6. Ajmal M, Jamal D, Quraishi MA (2000) *Anti Corros Methods Mater* 47:77
7. Quraishi MA, Jamal D, Sayeed T (2000) *J Am Oil Chem Soc* 77:265
8. Gasparac R, Martin CR, Stupnisek-Lisac E (2000) *J Electrochem Soc* 147:548
9. Zhang DQ, Gao LX, Zhu GD (2004) *Corros Sci* 46:3031
10. Wang L (2001) *Corros Sci* 43:2281
11. ASTM (1994) Standard practice for calculation of corrosion rate and related information from electrochemical measurements. Annual Book of Standards, G 102-89
12. Hoffmann K (1953) *Imidazole and its derivatives—Part-I: the chemistry of Heterocyclic compounds*. Interscience publishers Inc, New York, p 213
13. Hirozawa ST (1995) *Proceedings 8th European symposium on corrosion inhibition*, vol 1, Ferrara, Italy, p 25
14. Ashassi-Sorkhabi H, Shaabani B, Seifzadeh D (2005) *Electrochim Acta* 50:3446
15. Quraishi MA, Rawat J (2001) *Corrosion* 19:273
16. Rafiquee MZA, Khan S, Saxena N, Quraishi MA (2007) *Port Electrochim Acta* 25:419
17. Quraishi MA, Rafiquee MZA, Saxena N, Khan S (2007) *Ind J Chem Technol* 14:576
18. Jha LJ (1990) *Studies of the adsorption of amide derivative during acid corrosion of pure iron & its characterization*, PhD thesis, University of Delhi, 111
19. Breslin CB, Carrol WM (1993) *Corros Sci* 34:327
20. Khedr MGA, Lashien MS (1992) *Corros Sci* 33:137
21. Rehim SSA, Hassan HH, Amin MA (2001) *Mater Chem Phys* 70:64
22. Putilova IN, Balezin SA, Baranik UP (1960) *Metallic corrosion inhibitors*. Pergamon Press, New York, p 31
23. Gomma MK, Wahdan MH (1995) *Mater Chem Phys* 39:209
24. Schorr M, Yahalom J (1972) *Corros Sci* 12:867
25. Gomma GK, Wahdan MH (1995) *Ind J Chem Technol* 2:107
26. Orubite-Okorosaye K, Oforka NC (2004) *J Appl Sci Environ* 8:57
27. Atkins PW (1980) *Chemisorbed and physisorbed species, a textbook of physical chemistry*. University Press Oxford, Oxford, p 936
28. Quraishi MA, Khan S (2006) *J Appl Electrochem* 36:539
29. Juttner K (1990) *Electrochim. Acta* 35:1501
30. Houyi M, Chen S, Yin B, Zhao S, Liu X (2003) *Corros Sci* 45:867
31. Subramaniyam NC, Mayanna S (1985) *Corros Sci* 25:163
32. Wang HL, Fan HB, Zheng JS (2002) *Mater Chem Phys* 7:655
33. Quraishi MA, Mideen AS, Khan MA, Ajmal M (1994) *Ind J Chem Technol* 1:329